Morphology and mechanical stability of amyloid-like peptide fibrils

Patrick Mesquida · Christian K. Riener ·
Cait E. MacPhee · Rachel A. McKendry

Abstract Synthetic, amyloid-like peptide fibrils have recently attracted interest as a novel, potentially biocompatible material for applications in biotechnology and tissue-engineering. In this paper, we report atomic force microscopy (AFM) studies of the morphology and mechanical stability of fibrils self-assembled in vitro from the short peptide $TTR_{105–115}$, which serves as a model system for amyloid fibrils. It forms predominantly straight rods of approximately 1 μm in length and of diameters between 7 nm and 12 nm. We found polymorphism, with some fibrils exhibiting an unstructured morphology and others showing a regular, longitudinal surface pattern of 90 nm periodicity. Contact mode AFM-imaging in air was utilised to perform mechanical tests of individual fibrils on the nanometer scale with a defined, vertical force in the nN-range applied by the AFM-tip. Above 100 nN, all fibrils showed a permanent, mechanical deformation whereas below 40 nN, fibrils remained unaffected. Tapping-mode AFM-imaging in water led to fibril decomposition within 1.5 h whereas tapping-mode imaging in air left fibrils intact. Additional investigations by circular-dichroism spectroscopy showed that dispersed fibrils were structurally stable in aqueous solution between pH 3 and pH 8, and in sodium phosphate buffer of concentration between 50 mM and 1 M.

P. Mesquida (✉) · C. K. Riener · C. E. MacPhee ·
R. A. McKendry
London Centre for Nanotechnology and Department of
Medicine, University College London, 5 University Street,
London WC1E 6JJ, UK
e-mail: patrick.mesquida@kcl.ac.uk

Present Address:
P. Mesquida
Department of Mechanical Engineering, King's College
London, Strand WC2R 2LS, UK

Present Address:
C. E. MacPhee
Cambridge University Nanoscience Centre & Department
of Physics, Cavendish Laboratory, University of Cambridge,
Madingley Road, Cambridge CB3 0HE, UK

Introduction

In various disciplines of life sciences such as regenerative medicine, surgery or biotechnology, considerable efforts are being made in the search for biocompatible materials which exhibit specific, physical and chemical properties and simultaneously show the desired, biological tissue-response. Fibrous polypeptides have been identified as potential candidates for cell-scaffolds in tissue-engineering or for novel suture materials [1–4]. In Nature, fibrillar proteins are ubiquitous and serve a wide range of biophysical functions [5]. In cells for example, actin filaments and microtubules provide shape and motility and play an important role in cell division. In the extracellular matrix, collagen fibrils act as the scaffold on which cells can proliferate. Outside living organisms, protein fibres can be found, for example, in the form of spider silk, which exhibits a combination of outstanding mechanical properties such as a high tensile strength and a low specific weight [6].

Natural protein fibres such as collagen or silk are inherently difficult to synthesise in vitro from protein solutions. However, in recent years it has been discovered that amyloid-like peptide fibrils can easily be

produced by simple, chemical procedures in vitro [7, 8]. Amyloid fibrils, which typically have a diameter of a few nanometers, arise from the unfolding and aggregation of native proteins and polypeptides [9]. They show a characteristical "cross-beta" arrangement of β-sheets perpendicular to the fibril axis [10] and they have first been found in the form of amyloid-plaque deposits associated with protein-folding diseases such as Transmissible Spongiform Encephalopathies or Alzheimer's Disease [9].

A considerable number of proteins and synthetic polypeptides has been shown to form amyloid-like fibrils in vitro [3, 11]. The majority of these polypeptides are not related to any known disease and their amino-acid sequences are largely unrelated. Early speculation suggested that amyloid formation occured due to specific, amyloidogenic peptide sequence patterns. However, no such common patterns could be indentified and, furthermore, amyloid-like fibrils could even be produced from poly-amino-acids such as poly-L-lysine or poly-L-glutamic acid, which have no sequence patterns [12]. These findings indicate that the ability to form amyloid-like, β-sheet-rich fibrils is not a result of a pathological condition but a generic, thermodynamic property of any polypeptide molecule, independent of the amino-acid sequence [9].

We have recently shown that foreign sequences and non-peptide groups could be incorporated into synthetic fibrils of a given sequence [8], which could find applications in biomedical technologies such as tissue-engineering. Enhanced cell-adhesion on fibrils modified with functional sequences has recently been demonstrated by Kasai et al. [4]. As fibrils are often obtained in the form of hydrogels, applications could also be envisaged in cosmetics and pharmaceutics, where fibril gels with the desired physico-chemical properties could be produced.

For many potential applications, the mechanical properties of the peptide fibrils and their stability upon variations of the chemical milieu are important. As peptide fibrils have typical dimensions in the nanometer range, atomic force microscopy (AFM) is an ideal tool to directly test the mechanical properties of individual fibrils.

In this paper, we report AFM-studies of the mechanical stability of peptide fibrils produced from the synthetic peptide TTR$_{105–115}$ (YTIAALLSPYS) in air and liquid. This short peptide, which corresponds to the G β-strand of the human plasma protein transthyretin, has been chosen because it readily forms well-defined fibrils at low pH [8], foreign peptide sequences can be incorporated [8] and the molecular structure of the fibrils has been elucidated

to a great extent [13, 14]. In addition to AFM, spectroscopic investigations of the structural stability of TTR$_{105–115}$-fibrils upon pH and salt concentration variations in solution are presented.

Experimental methods and sample preparation

TTR$_{105–115}$ peptide was acquired by purchase (CS Bio Company Inc., Menlo Park CA, USA) or synthesised in our lab by standard Fmoc synthesis (PS3 automated peptide synthesiser, Protein Technologies Inc, Tucson AZ, USA). It was transformed into fibrils by dissolving 10 mg/ml peptide in an aqueous, 20 vol% CH$_3$CN-solution, which was adjusted to pH 2 by adding a small amount of concentrated HCl. The solution was subsequently incubated for 2 days at 37°C, after which it formed a highly concentrated suspension as described in previous works [8, 15]. The fibrils were then diluted in deionised (DI) water (specific resistivity >15MΩ cm, Elgastat Maxima, Elga Ltd., High Wycombe, UK) at volume-to-volume ratios indicated below. For AFM-imaging and mechanical testing, the fibrils were adsorbed on mica by immersing freshly cleaved mica pieces (Agar Scientific Ltd, Stansted, UK) into the diluted fibril suspensions for 1–2 min and subsequently rinsing the samples with copious amounts of DI-water and drying the samples in a stream of dry nitrogen. As a comparison in terms of fibril morphology, bovine insulin fibrils were produced by dissolving 11 mg/ml of the protein (Sigma-Aldrich Co, St.Louis MO, USA) in DI-water adjusted to pH 2 by adding a small amount of HCl and incubating the solution at 70°C for 2 days. In some of the experiments, colloidal Au particles (Sigma-Aldrich Co, St.Louis MO, USA) of 21.5 nm diameter were deposited on mica prior to fibril adsorption, to serve as a reference [15].

AFM-imaging and AFM-based mechanical-testing was performed using a Digital-Instruments Dimension 3,100 AFM or a Digital-Instruments MultiMode AFM (Veeco Metrology LLC, Sta.Barbara CA, USA) with standard, silicon or silicon nitride tips (NSC12, MikroMasch, Madrid, Spain; OMCL-AC160TS, Olympus Corp., Tokyo, Japan; OTR8 and MSCT Microlevers, Veeco Metrology LLC, Sta.Barbara CA, USA). All experiments were performed in air under ambient conditions unless otherwise indicated. For routine AFM-imaging, tapping-mode has been employed, which generates a lower mechanical force on the samples than contact mode. The latter was used for mechanical-testing because a defined and quantifiable force can be applied to the samples.

The stability of dispersed fibrils in suspension was investigated by Circular-Dichroism (CD) spectroscopy using a Jasco J-810 spectropolarimeter (Jasco Inc, Easton, MD, USA) with a 1-mm-path-length quartz cuvette. The 10-mg/ml-suspension was diluted at a volume-to-volume ratio of 1:40 in sodium–phosphate buffers (Na_2HPO_4:NaH_2PO_4) of different concentrations and pH and the spectra were acquired by averaging over 5 scans for each spectrum.

Results and discussion

Morphology

The topographical AFM images in Fig. 1 show typical morphologies of amyloid-like fibrils. Fibrils formed from $TTR_{105-115}$ are unbranched, predominantly straight rods with lengths of up to approximately 1 μm (Fig. 1a). Randomly adsorbed individual fibrils and bundles of fibrils can be discerned on the mica substrate. Figures 1b, c show high-resolution images of individual $TTR_{105-115}$-fibrils. The example shown in Fig. 1b does not possess any obvious topographical structure whereas the fibril in Fig. 1c shows a clear, periodic pattern on its surface, which can be attributed to protofilaments wound around each other, consistent with commonly accepted, structural models for amyloid fibrils [16]. The samples shown in Figs. 1b, c were prepared using different batches of $TTR_{105-115}$-peptide [(b) = purchased, (c) = synthesised in our lab], which could account for the polymorphism. Similar variations

have been reported in the literature for other amyloid precursor proteins [17, 18]. One might speculate that different amounts of residual, non-peptide reagents used during the peptide synthesis could affect the arrangement of protofilaments in the fibrils. It has actually been shown for another amyloid-forming peptide that even subtle variations of the physical fibril growth conditions, such as agitation of the peptide solutions, can affect their morphology [19].

A longitudinal profile of the patterned fibril is shown in Fig. 1d. The periodicity of the pattern is approximately 90 nm with the protrusions and indents varying between 11 nm and 8 nm, respectively, in height. For those fibrils that did not show a topographical pattern, an average diameter of 9.7 nm ± 1.9 nm was found. It should be noted that this interpretation of AFM-measurements is under the assumption that the fibrils have a circular cross-section and preserve this shape when adsorbed on mica. In this case, the height measured by AFM rather than the apparent width corresponds to the fibril diameter because of the tip-broadening effect in AFM-imaging. Although tapping-mode-imaging is generally considered to be a very gentle form of imaging biological objects, the tip still exerts a small force of the order of 0.1–1 nN on the sample [20], which could affect the measured z-height. However, reducing the tapping-mode setpoint from 80% to 10% of the free amplitude did not lead to any significant variations of the measured z-height or of the image quality of individual fibrils, which indicates that the force applied in tapping-mode in air is low enough to allow non-perturbative imaging.

Fig. 1 Morphological characterisation of peptide fibrils by atomic force microscopy (AFM). $TTR_{105-115}$-fibrils [except (**e**) and (**f**) = insulin fibrils] diluted in DI-water and adsorbed on mica, tapping-mode-imaging of topography, (**a**) amplitude image, arbitrary z-scale, 1:20 dilution, (**b**) height image, z-scale = 20 nm, 1:20 dilution, white line = representative fast-scan line, (**c**) height image, z-scale = 30 nm, 1:25 dilution, dashed line = longitudinal profile shown in (**d**), (**e**) insulin fibrils, amplitude image, arbitrary z-scale, 1:200 dilution, (**f**) single insulin fibril, height image, z-scale = 20 nm, 1:2,000 dilution
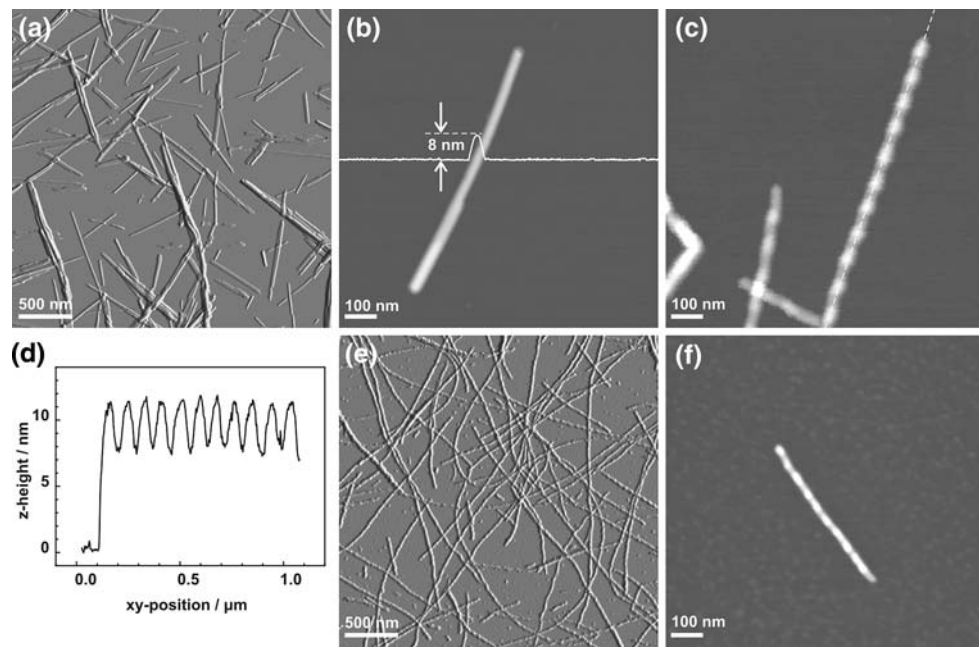
Figure 1e shows fibrils from bovine insulin adsorbed on mica for comparison. Insulin fibrils are longer and show a more curved shape and less tendency to form bundles than $TTR_{105-115}$-fibrils. This is an indication that insulin fibrils are mechanically more flexible than $TTR_{105-115}$-fibrils. Furthermore, insulin fibrils always exhibit a topographical, periodic pattern as shown in Fig. 1f with a repeat distance of ca. 50 nm, which is in agreement with cryo-transmission electron microscopy data [16].

Mechanical stability in air

In air, a mechanical alteration of $TTR_{105-115}$-fibrils could not be observed when performing tapping-mode AFM. However, under high loads we found significant, permanent changes of the morphology when imaging the fibrils in contact mode. Therefore, contact-mode-imaging has been utilised to perform direct mechanical-testing of individual $TTR_{105-115}$-fibrils by monitoring the changes of the morphology before and after applying a defined force.

Three consecutive contact mode scans of an individual fibril were taken: First, the fibril was imaged at the lowest possible force at which a stable image could be obtained with no sample damage (Fig. 2a). Then—without withdrawing the tip—a second scan was performed with the same force, except on specific scan-lines (denoted by the arrows from 1 to 9 in Fig. 2b), where the force was temporarily increased by a defined amount by increasing the contact mode setpoint. This led to nanometer-sized indentations or "cuts" in the fibril. Finally, a third image was taken, again at the lowest possible force, in order to visualise the indentations (Fig. 2b).

The depth of the indentations was measured by analysing longitudinal cross-sections of the fibrils (Fig. 2c). The experiments were performed with cantilevers of different spring constant, k, which had been individually calibrated by the thermal-tuning
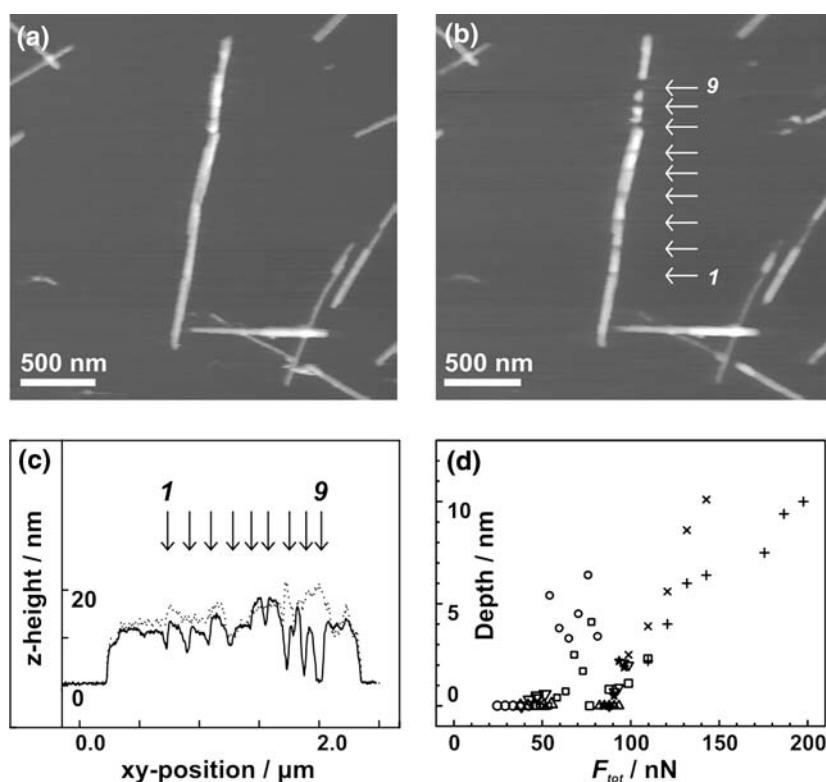

Fig. 2 Direct mechanical testing of $TTR_{105-115}$-fibrils by contact mode imaging in air. Fibrils diluted 1:40 in DI-water and adsorbed on mica, atomic force microscopy (AFM)-cantilevers used = MSCT Microlever E, spring constant $k = 0.268$ N/m (calibrated with the thermal-tune function of the Digital Instruments Nanoscope IV software), (**a**) height image before indentation, z-scale = 30 nm, (**b**) height image after indentation, z-scale = 30 nm, the positions of the indentation scans are indicated by arrows, 1 = first indentation, 9 = ninth and last indentation, (**c**) longitudinal profiles of fibril shown in (**a**) = dotted line and (**b**) = continuous line, (**d**) indentation depth vs. total indentation force, F_{tot}, analysis of 11 randomly chosen fibrils, each symbol represents data from one fibril

method for each cantilever [21]. In addition to the spring force,

$$F_S = k \cdot d,$$

where d is the cantilever deflection, there is always a substantial adhesion force, F_A, between AFM-tip and sample surface, especially on hydrophilic samples such as mica, due to a thin water layer present in air under ambient conditions. This force is typically larger than 10 nN. It can easily be determined by measuring deflection-vs.-z-position force curves and analysing the adhesion peak upon retraction of the tip [22]. The vertical (normal) component of the total force, F_{tot}, applied to the fibril was then calculated by adding the adhesion force to the spring force of the cantilever,

$$F_{tot} = F_S + F_A.$$

Figure 2c shows an example of a longitudinal profile of an individual TTR$_{105-115}$-fibril (continuous line), in which 9 indentations have been made. The dotted line is the profile before the indentation was performed. The force, F_S, was increased by a defined amount on selected scan-lines from position 1 to 9. Figure 2c shows how the indentations become deeper upon increasing force. Although relatively soft cantilevers were used (0.069 N/m $\leq k \leq$ 0.268 N/m) the lower experimental limit of F_{tot} was given by F_A, which was always found to be in the range of 20–30 nN. Figure 2d shows depth-of-indentation of 11 randomly chosen, individual fibrils vs. F_{tot}. The minimum force necessary to indent the fibrils was approximately 40 nN. Upon applying tip loads of between 40 nN and 100 nN, fibrils could be indented but the minimum force required was found to be different for different fibrils. Above $F_{tot} \approx 100$ nN an indentation was always observed. Similar AFM-manipulation experiments to investigate the mechanical properties of protein fibrils have recently been reported [23, 24]. Lateral stretching was observed for intermediate filaments [23] and a non-linear dependence of the rupture force on the fibril diameter was obtained for fibrin [24]. In our experiments we did not observe any lateral displacement or stretching, which indicates that the adsorption force of TTR$_{105-115}$-fibrils on mica is stronger than the intermolecular forces that hold individual fibrils together. However, from our measurements alone, the exact indentation mechanism cannot be determined, that is, whether material is simply removed by the AFM-tip or whether some molecular rearrangement takes place in the fibril.

Mechanical stability in water

In a liquid environment, non-destructive contact mode imaging of soft materials is usually facilitated by the lack of a thin water layer on the surface of the sample and hence the lack of an adhesion force in the nN-range. However, contact-mode-imaging of TTR$_{105-115}$-fibrils was not possible in water even by using forces as low as approximately 0.5 nN, which can be explained by a reduction of the mechanical stability of the fibrils in water. Tapping-mode-imaging, on the other hand, was possible by careful adjustment of the setpoint to achieve the lowest possible perturbation. A precise, quantitative determination of the force applied to a sample in tapping-mode is not as straightforward as in contact mode because the cantilever oscillates above the sample and "taps" the fibrils at a given frequency. In general, the force on the sample is increased by reducing the setpoint and thereby "forcing" the cantilever into a smaller oscillation amplitude at a given drive amplitude. San Paulo and Garcia analysed theoretically the tip-sample interaction forces in tapping-mode [20] and provided mathematical expressions taking into account tip oscillation parameters such as the resonance frequency or the tip quality factor. With formula (5) and (7) from [20] we can estimate the average tip-sample force for the cantilevers used in our experiments (spring constant = 0.15 N/m, quality factor $\approx$1–4, resonance frequency = 8.24 kHz, free amplitude $\approx$25 nm, tapping-mode setpoint $\approx$20 nm) to values <1 nN.

Figure 3 shows a sequence of 6 consecutive tapping-mode images of a bundle of TTR$_{105-115}$-fibrils adsorbed on mica and immersed in DI-water (pH $\approx$ 5–6). Amplitude images are shown because of their better contrast and because quantitative height information is not needed here. Each image took ca. 4 min. to complete after which the scanning has been paused for a given time and then resumed again at the times indicated in Fig. 3. All images were recorded at the same setpoint. Colloidal Au particles have been deposited on the mica sample before adsorbing TTR$_{105-115}$-fibrils to serve as a reference for finding the same position again in consecutive images. Figure 3 shows that the fibril bundle dissolves within approximately 1.5 h. This effect is caused by the AFM-tip as control experiments with fibrils immersed in water, but without being scanned by AFM, did not show any significant decomposition in the period of a few hours. However, in water, the fibrils seem to be mechanically "weakened", as in comparison TM-imaging in air did not show any decomposition. It is also interesting to note that fibrils did not move on the

Fig. 3 Direct mechanical testing of TTR$_{105-115}$-fibrils by tapping-mode-imaging in DI-water. Sequence of 6 consecutive scans, 1:5 dilution in DI-water, adsorbed on mica, on which colloidal Au nanoparticles were previously deposited (s. text, sample preparation), amplitude images, arbitrary z-scale, silicon nitride cantilevers [Olympus OTR8, resonance frequency in air (water) = 24 kHz (8 kHz)], tapping-mode setpoint approximately 70% of the free amplitude, start time of each image with respect to first image (0 min) as indicated, sample was continuously immersed in DI-water during measurement
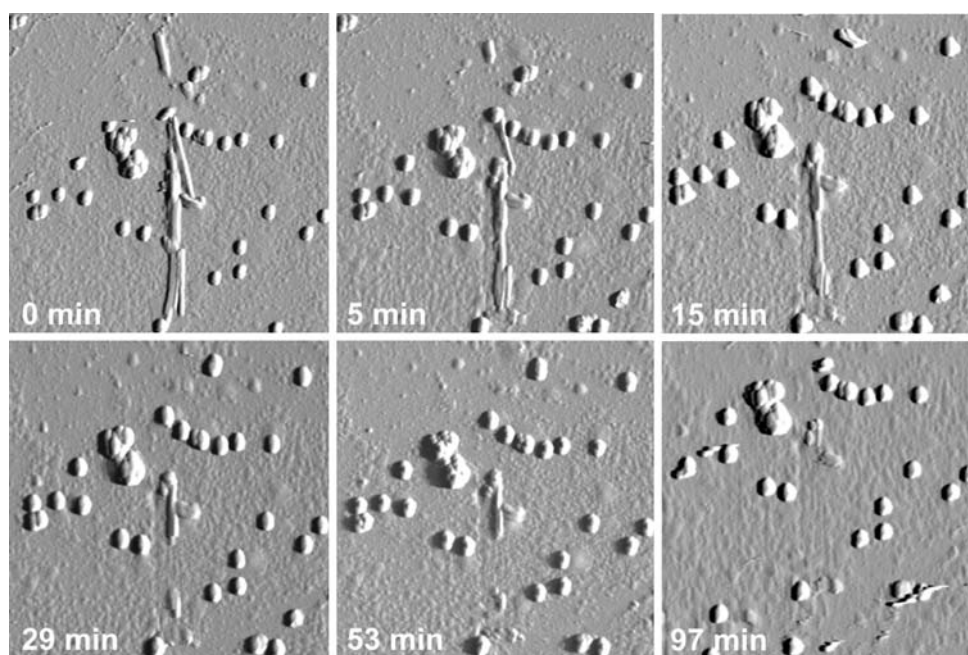
substrate, which can be explained by adsorption forces on mica which are stronger than the intrafibrillar forces that preserve the fibril structure.

Chemical stability in suspension

Although the decomposition of TTR$_{105-115}$-fibrils in DI-water could be attributed to the mechanical influence of the tip, a possible effect of the solvent conditions on the structural integrity of the fibrils cannot be excluded as the conformation of many polypeptides depends on pH and electrolyte concentration of the solvent.

To investigate the structural stability of TTR$_{105-115}$-fibrils, 10-mg/ml-suspensions were diluted in sodium phosphate buffer solutions of different pH or concentrations and investigated by CD-spectroscopy. The characteristic shapes of the CD-curves in Fig. 4a with the small, local minimum at 235–240 nm show that the fibrils were not significantly affected by pH in the range from acidic (pH = 3) to slightly basic (pH = 8) condi-

tions. Similar measurements shown in Fig. 4b reveal that the fibrils are also stable at varying phosphate buffer concentrations, ranging from 50 mM to 1 M at pH = 7. These measurements indicate that self-assembled peptide fibrils are stable upon variations of the chemical environment.

Summary and conclusions

We have reported AFM studies of self-assembled, amyloid-like peptide fibrils produced in vitro from the short peptide TTR$_{105-115}$. The fibrils were typically straight rods of up to 1 μm in length and a diameter in the range of 7–12 nm. Polymorphism was observed, which is likely to reflect the different arrangement of protofilaments as constituents of the fibrils. These variations could be caused by small differences of the fibril formation conditions. Although TTR$_{105-115}$ is not specifically implicated in any known amyloid-disease there is some evidence that different morphologies of

Fig. 4 CD-spectra of TTR$_{105-115}$-fibril suspensions. Dilution of 1:40 in sodium-phosphate buffer except for pH = 3, (**a**) spectra at different pH, phosphate concentration = 0.1 M. For pH = 3 fibrils were diluted 1:40 in DI-water instead of phosphate buffer, (**b**) spectra at different phosphate concentrations, pH = 7
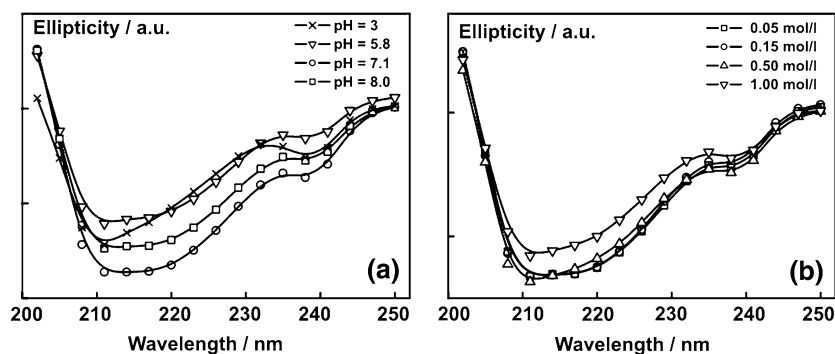
fibrils formed from the same amyloidogenic protein could account for different levels of toxicity in case of amyloid fibrils that are linked to well-known diseases such as Alzheimer's disease.

Further to morphological characterisation we have performed contact mode AFM-imaging in air as a means to directly perform mechanical tests of individual fibrils on the nanometer scale by applying a defined, normal force in the nN-range. Above 100 nN the fibrils could always be indented and the degree of permanent, mechanical deformation increased with the force applied. Below 40 nN the fibrils were unaffected. Tapping-mode AFM-imaging in water led to decomposition of the fibrils, which could be attributed to structural weakening of the hydrated form. The exact cause of this effect is not known, however, it could be that the mechanical excitation of the AFM-tip during the measurement causes an acoustic wave in the water which might disrupt the fibrils. This is supported by the fact that tapping-mode-imaging in air and simply immersing the fibrils in water without AFM-imaging did not lead to any decomposition. This was confirmed by spectroscopic investigations, which showed that the fibrils were structurally stable upon variations of pH and salt concentration of the solvent, which presents a significant advantage for processing fibrils in possible pharmaceutical or biotechnical applications. Further systematic, nanomechanical studies of amyloid-like fibrils are essential for future applications in tissue-engineering.

References

1. S. ZHANG, *Nat. Biotechnol.* **21**(10) (2003) 1171
2. A. AGGELI, N. BODEN and S. ZHANG (eds) *Self-Assembling Peptide Systems in Biology, Medicine and Engineering*, 1st edn (Dordrecht, Norwell: Kluwer Academic Publishers, 2001)
3. C. E. MACPHEE and D. N. WOOLFSON, *Curr. Opin. Solid State Mater. Sci.* **8**(2) (2004) 141
4. S. KASAI, Y. OHGA, M. MOCHIZUKI, N. NISHI, Y. KADOYA and M. NOMIZU, *Biopolymers (Peptide Science)* **76** (2004) 27
5. T. D. POLLARD and W. C. EARNSHAW, *Cell Biology* (London: W. B. Saunders, 2002)
6. M. ELICES, J. PEREZ-RIGUEIRO, G. R. PLAZA and G. V. GUINEA, *JOM The Minerals, Metals & Materials Society's Monthly Membership Journal* **57**(2) (2005) 60
7. J. I. GUIJARRO, M. SUNDE, J. A. JONES, I. D. CAMPBELL and C. M. DOBSON, *Proc. Natl. Acad. Sci. U.S.A.* **95** (1998) 4224
8. C. E. MACPHEE and C. M. DOBSON, *J. Am. Chem. Soc.* **122** (2000) 12707
9. C. M. DOBSON, *Phil. Trans. R. Soc. Lond.* **B356** (2001) 133
10. M. SUNDE and C. C. F. BLAKE, *Adv. Protein Chem.* **50** (1997) 123
11. A. M. FERNANDEZ, F. ROUSSEAU, J. SCHYMKO-WITZ and L. SERRANO, *Nat. Biotechnol.* **22**(10) (2004) 1302
12. M. FÄNDRICH and C. M. DOBSON, *EMBO J.* **21**(21) (2002) 5682
13. C. P. JARONIEC, C. E. MACPHEE, N. S. ASTROF, C. M. DOBSON and R. G. GRIFFIN, *Proc. Natl. Acad. Sci. U.S.A.* **99** (2002) 16748
14. C. P. JARONIEC, C. E. MACPHEE, V. S. BAJAJ, M. T. MCMAHON, C. M. DOBSON and R. G. GRIFFIN, *Proc. Natl. Acad. Sci. U.S.A.* **101** (2004) 711
15. P. MESQUIDA, D. L. AMMANN, C. E. MACPHEE and R. A. MCKENDRY, *Adv. Mater.* **17**(7) (2005) 893
16. J. L. JIMENEZ, E. J. NETTLETON, M. BOUCHARD, C. V. ROBINSON, C. M. DOBSON and H. R. SAIBIL, *Proc. Natl. Acad. Sci. U.S.A.* **99** (2002) 9196
17. H. H. BAUER, U. AEBI, M. HANER, R. HERMANN, M. MULLER, T. ARVINTE and H. P. MERKLE, *J. Struct. Biol.* **115**(1) (1995) 1
18. C. S. GOLDSBURY, G. J. S. COOPER, K. N. GOLDIE, S. A. MULLER, E. L. SAAFI, W. T. M. GRUIJTERS, M. P. MISUR, A. ENGEL, U. AEBI and J. KISTLER, *J. Struct. Biol.* **119**(1) (1997) 17
19. A. PETKOVA, R. D. LEAPMAN, Z. GUO, W.-M. YAU, M. P. MATTSON and R. TYCKO, *Science* **307** (2005) 262
20. A. S. PAULO and R. GARCIA, *Phys. Rev. B* **66**(4) (2002) Art.-No. 041406
21. H.-J. BUTT and M. JASCHKE, *Nanotechnol.* **6** (1995) 1
22. K. D. JANDT, *Surf. Sci.* **491** (2001) 303
23. L. KREPLAK, H. BAR, J. F. LETERRIER, H. HERR-MANN and U. AEBI, *J. Mol. Biol.* **354**(3) (2005) 569
24. M. GUTHOLD, W. LIU, B. STEPHENS, S. T. LORD, R. R. HANTGAN, D. A. ERIE, R. M. TAYLOR and R. SUPERFINE, *Biophys. J.* **87**(6) (2004) 4226